Journal of Energy Storage 48 (2022) 103999

Contents lists available at ScienceDirect

Journal of Energy Storage

journal homepage: www.elsevier.com/locate/est

Research Papers

Optimizing the operation of energy storage embedded energy hub concerning the resilience index of critical load

Jafar Khayatzadeh, Soodabeh Soleymani *, Seyed Babak Mozafari, Hosein Mohammadnezhad Shourkaei

Department of Electrical Engineering, Science and Research Branch, Islamic Azad University, Tehran, Iran

ARTICLE INFO

Keywords:
Energy hub
Energy storage
Resiliency
Operation costs
Energy not supplied
Critical load
Non-critical load

ABSTRACT

Dealing with high-impact events in energy hubs requires increasing resistance and restoration capability in multi-carrier energy systems. Assessing resilience as an essential and high priority measure must be done to ensure the optimal and economical operation of the energy hub. Thus, this paper introduces a cost-based optimization model of the energy hub that contains storage and considers resilience constraints and other general constraints. In this methodology, loads are categorized as critical and non-critical. The approach defines the highest priority for supplying the critical loads, whereas interruptions in non-critical loads must be minimized. That in this context, storages play a vital role. Four scenarios are investigated as normal situations and contingency cases. The contingency scenarios examine energy carrier interruptions such as electricity, gas, and heat input in an energy hub system. The mathematical model of this problem is founded based on a Mixed Integer Nonlinear Programming (MINLP), which DICOPT solver implements in GAMS. Mentioned model is evaluated by simulation of different case studies for the given energy hub test system. The trade-off between increasing critical load resiliency and reducing total costs is investigated. The results show that as critical load flexibility increases, total costs increase. In the worst-case scenario, only up to 13% of the total load can also be considered as critical load. Moreover, in different scenarios, the results demonstrate that using storage devices helps to increase resiliency Furthermore, in severe events, using storage devices has an increasing trend.

1. Introduction

1.1. Motivation

With the growth of human societies and the industrialization of countries, energy supply of industrial loads is one of the important issues. The Load interruption creates economic and societal difficulty, resulting in customer dissatisfaction. Therefore, in recent years, a general framework has been proposed combined with various energy carriers that perform the conversion and store process to supply the required load, called the energy hub [1]. Furthermore, Security protection of infrastructure systems such as electricity network against normal events with low effect and high probability has always been considered by designers and operators [2]. However, the performance of these systems is seriously disrupted against severe events. Therefore, it is necessary to study the system's behavior in the event of severe accidents and, if necessary, take the necessary measures to solve the problems. This behavior is known as a new feature called infrastructure system resiliency that refers to the temporal performance of a system including resistance, vulnerability, and reversibility facing a severe event [3]. In this regard, this paper discusses how to operate the energy hub while minimizing the feed costs of critical and non-critical loads (CNCLs) and the utilization costs of the storage device in optimal condition. Additionally, the main objective of this approach is to increase resilience by feeding the critical loads. Therefore, reducing the total energy hub cost while improving the resilience of critical loads is challenging.

1.2. Literature survey

Lu et al. [4] presents an optimal load distribution approach for a community energy hub that reduces the cost of the energy hub. The mentioned cost includes cost of operation and the cost of carbon emissions. Thermal and electrical demand response (DR.) considered in this method; furthermore, a random access model is proposed for large-scale electric vehicles. The simulation result demonstrates that the total costs

* Corresponding author.
E-mail address: s.soleymani@srbiau.ac.ir (S. Soleymani).

https://doi.org/10.1016/j.est.2022.103999
Received 9 October 2021; Received in revised form 27 December 2021; Accepted 6 January 2022
Available online 13 January 2022

Nomenclature

Indices

t	counter for the time
j	counter for the number of equipment
π_h_t	input heat price
$Pout\_e_t$	total electrical load
P_R	output load after the event
$Pout\_h_t$	total heating load
$Pout\_c_t$	total cooling load
$\pi\_ES\_e_{j.t}$	price of j^{th} electrical energy storage
$\pi\_ES\_h_{j.t}$	price of j^{th} heating energy storage
$\pi\_ES\_c_{j.t}$	price of j^{th} cooling energy storage
Pen_e_t	penalty factor for the electrical load that is not fed
Pen_h_t	penalty factor for the heating load that is not fed
Pen_c_t	penalty factor for the cooling load that is not fed

Scalars

α	price coefficient for feed critical loads
β	price coefficient for feed non-critical loads
η_Se	electrical storage. efficiency
η_Sh	heating storage. efficiency
η_Sc	cooling storage. efficiency
L_ESe	internal losses of .electrical. storage
L_ESh	internal losses of heating. storage
L_ESc	internal losses of cooling. storage
η_e	transformer efficiency
η_chp_e	electrical efficiency. of CHP
η_chp_h	heating efficiency. of CHP
η_cchp_e	electrical efficiency. of CCHP
η_cchp_h	heating efficiency. of CCHP
η_cchp_c	cooling efficiency. of CCHP
η_b	efficiency of boiler
η_H	efficiency of heater
$P\_e_j^{min}$	minimum value for input power of. transformer
$P\_e_j^{max}$	maximum value for input. power of transformer
P_chp^{min}	minimum value for input. power of CHP
P_chp^{max}	maximum value for input. power of CHP
P_cchp^{min}	minimum value for input. power of CCHP
P_cchp^{max}	maximum value for input. power of CCHP
P_b^{min}	minimum value for input. power of Boiler
P_b^{max}	maximum value for input. power of the boiler
P_H^{min}	minimum value for input. power. of the heater
P_H^{max}	maximum value for input power. of the heater
Sin_e^{min}	minimum value for input power. of electrical storage
Sin_e^{max}	maximum value for input power. of electrical storage
$Sout\_e^{min}$	minimum value for output power. of electrical storage
$Sout\_e^{max}$	maximum value for output power. of electrical storage
ES_e^{min}	minimum value for energy of .electrical storage
ES_e^{max}	maximum value for energy of .electrical storage
Sin_h^{min}	minimum value for input power of .heating storage
Sin_h^{max}	maximum value for input power of heating storage
$Sout\_h^{min}$	minimum value for output power of heating storage
$Sout\_h^{max}$	maximum value for output power of heating storage
ES_h^{min}	minimum energy of heating storage
ES_h^{max}	maximum energy of heating storage
Sin_c^{min}	minimum value for input power of cooling storage
Sin_c^{max}	maximum value for input power of cooling storage
$Sout\_c^{min}$	minimum value for output power of cooling storage
$Sout\_c^{max}$	maximum value for output power of cooling storage

Abbreviations

NC-S	non-critical loads that are fed
NC-NS	non-critical loads that are not fed
MECS	multi-energy-carrier system
CNCL	critical and Non-critical loads

Parameters

π_e_t	input electricity price
π_g_t	input gas price
ES_c^{max}	maximum energy of cooling storage

Binary variable

$I\_e_{j.t}$	j^{th} transformer status (in service=1,else=0)
$I\_chp_{j.t}$	j^{th} CHP status (in service=1,else=0)
$I\_cchp_{j.t}$	j^{th} CCHP status (in service=1,else=0)
$I\_b_{j.t}$	j^{th} boiler status (in service=1,else=0)
$I\_H_{j.t}$	j^{th} heater status (in service=1,else=0)
$I\_ES\_e_{j.t}$	j^{th} electrical energy storage status (in service=1,else=0)
$I\_ES\_h_{j.t}$	j^{th} heating energy storage status (in service=1,else=0)
$I\_ES\_c_{j.t}$	j^{th} cooling energy storage status (in service=1,else=0)

Variable

OC	total operation cost
$OC1 \sim OC16$	operation cost of converters
STC	operation cost of storage devices
$PenC$	penalty cost of not supplied non-critical load
Pin_e_t	total input electrical energy
Pin_g_t	total input gas
Pin_H_t	total input heat
$P\_e_{j.t}$	input electrical energy to j^{th} transformer
P_chp	input energy to j^{th} CHP
$P\_cchp_{j.t}$	input energy to j^{th} CCHP
$P\_b_{j.t}$	input energy to j^{th} boiler
$P\_H_{j.t}$	input energy to j^{th} heater
$P\_Ex\_e_{j.t}$	output electrical energy from j^{th} transformer
$P\_Ex\_chp\_e_{j.t}$	output electrical energy from j^{th} CHP
$P\_Ex\_chp\_h_{j.t}$	output heating energy from j^{th} CHP
$P\_Ex\_cchp\_e_{j.t}$	output electrical energy from j^{th} CCHP
$P\_Ex\_cchp\_h_{j.t}$	output heating energy from j^{th} CCHP
$P\_Ex\_cchp\_c_{j.t}$	output cooling energy from j^{th} CCHP
$P\_Ex\_b_{j.t}$	output heating energy from j^{th} boiler
$P\_Ex\_H_{j.t}$	OUTPUT HEATING ENERGY FROM j^{th} heater
$P\_e\_c_t$	electrical critical Load
$P\_e\_ncs_t$	electrical non-critical Load that is fed
$P\_e\_ncns_t$	electrical non-critical Load that is not fed
$P\_h\_c_t$	heating critical Load
$P\_h\_ncs_t$	heating non-critical Load that is fed
$P\_h\_ncns_t$	heating non-critical Load that is not fed
$P\_c\_c_t$	cooling critical Load
$P\_c\_ncs_t$	cooling non-critical Load that is fed
$P\_c\_ncns_t$	cooling non-critical Load that is not fed
$R(T).R1(T)$	resiliency index
$Sin\_e(t)$	input power to electrical storage
$Sout\_e(t)$	output power from electrical storage
$Sin\_h(t)$	input power to heating storage
$Sout\_h(t)$	output power from heating storage
$Sin\_c(t)$	input power to cooling storage
$Sout\_c(t)$	output power from cooling storage
$ES\_e(t)$	electrical energy storage
$ES\_h(t)$	heating energy storage
$ES\_c(t)$	cooling energy storage
$v1$	share of input gas to CHP
$v2$	share of input gas to CCHP
A_{mn}	coupling matrix
$CNCL_e$	critical and non-critical electrical loads
$CNCL_h$	critical and non-critical haeting loads
$CNCL_c$	critical and non-critical cooling loads

can be effectively reduced by deciding on a coordinated charge/discharge mode for EVs. Beside, by implementing demand response programs, the total cost of consumers can be further reduced. In this paper, despite reducing costs in the energy hub, the increase of resilience and system losses are not considered. In [5], multiple energy carrier microgrids examine resilience-promoting proactive scheduling. The availability index equals the sum of the electric and thermal energy storage, which must be increased. The objective function is to grow the supply of non-critical loads in the network. Thus, there is a trade-off between the two conflicting objective functions (availability index and load supply). In this paper, economic analysis has not been done with a cost minimization approach despite the study of resilience in a system. In [6], optimal operation of multi-energy carriers using the concept of energy hub with the uncertainty of wind power plants has been investigated. The objective function in this paper is defined as the minimization of operation costs; GAMS software is used to solve the problem. Furthermore, the uncertainty of wind units is considered a Weibull function at the input of the system. Also, Load uncertainty at the energy hub output is modeled as a normal distribution. In [7], the location of the Energy Storage Systems for increasing resilience against earthquakes is studied. The objective function is to maximize the energy capacity of storage devices to supply critical loads. The test system is one of the electricity distribution networks in Tehran. Beside the approach demonstrates a linear programming (LP) technique. As a result, resilience is improved by up to 40% [8]. Presents a new method that illustrate the resiliency in microgrids using Battery Swapping Stations (BSSs). An efficient bi-level model is presented in which microgrid (MG) solves the high level of the proposed model to report unsupplied loads and excess energy to the BSSs coordinator during islanding. BSSs coordinator will do the lower-level problem to the public the prices of energy transactions for various plans to the MG. The result shows the unsupplied loads cost of MG considering the value of lost loads was minimized and the resiliency of MG improve while used the BSSs [9]. Emphasizes scheduling the integrated plug-in wind power plant and hybrid electric vehicle in the day-ahead market.

Moreover, an offering/bidding and scheduling strategy that uses a two-stage bi-level hybrid stochastic-robust process is presented. The cost model of linear battery erosion with semi-correct variables is also included to show the battery erosion of PHEVs. To do this, k-means clustering is used to locate the various fleets of plug-in hybrid electric vehicles, and pollutants pose a high-level problem. Operating costs and the cost of power purchased in the day-ahead market are included in the cost objective data sets containing uncertain information, such as arrival/departure timings of vehicle fleets and their travel distances. The lower-level is done by the market operator that has the objective of maximizing social welfare. The result shows that the price-maker player can change the locational marginal price up to 4.4%, while the emissions can be reduced by 40%. In [10], a kind of node reaction of multi-energy carrier systems (MECS) against storms was suggested that nodal indices are defined to quantify the resiliency of multi-energy-carrier systems. In this regard and first step, the multi-phase performance curve is used to describe the response behavior of MECSs at various phases under the effects of storms. Afterward, a special model for optimum energy flow is proposed to minimize the effects of storms. In addition, node resiliency indices are proposed for several energy carriers to determine the degree of resilience in MESs. The results show that the resilience performance levels of MESs in separate areas differ from the effects of storms. In [11], energy hub models are proposed for areas with major changes in ambient temperature. Load and electricity prices are presented as uncertainties in the related model, and studies have shown that the purchased energy is reduced due to uncertainty.

In [12] proposed a pattern to decrease operating costs in the energy hub. Reliability indicators are reviewed and the cost of fines is not taken into account for expected energy supply. In [13] proposed a novel approach estimating the level of renewable penetration, and there is a compromise between increasing the penetration of renewable units and reducing the cost of the system. An algorithm is presented to diagnose the effect of renewable penetration level on the scheduling of power to gas (P.t.G) and gas-fired generation (G.f.G) equipment.

Najafi et al. [14] uses several private MGs to improve the resilience of water-electricity distribution systems. Also, resilience is defined as increasing users' access to electricity and water after natural disasters. MGs restore interrupted loads in distribution networks. In this method, a stochastic energy program is designed for MG that specifies the amount of energy that can be delivered to distribution systems by considering local loads' reliability. The Distribution System Operator (DSO) receives MGs' bid strategy for energy blocks. Then, the DSO chooses the best plan to restore interrupted loads considering inaccessibility values to electricity, water, and damage. This reference is considering the modified IEEE 33-bus distribution network for the case study. The results represented enhanced resilience against natural disasters.

New scheme of Thyristor Controlled Series Compensators (TCSC)-based damping controller has been proposed in [15] for damping inter-area oscillations in bulk power systems based on a wide area measurement. This reference represents a scheme that provides a three-phase adaptive phase using real-time operation mode. A dynamic clustering-based technique is presented in the first stage for assessing the inter-area oscillations of the system, which, in real-time, identifies the corresponding oscillating areas. Based on a practical case study from Iran National Power Grid, a reduction-order model was developed to assess the effectiveness of the damping controller scheme. Damping controllers dynamics have been examined by reducing the size and complexity of systems.

An optimization framework for the energy hub operation is designed to obtain the optimal capacity of distributed energy sources concerning environmental issues. In addition to the uncertainty of heat and electricity loads, the intermittent behavior of wind resources and solar radiations is also expressed as uncertainty factors in the problem. The results proved that considering these indicators leads to a further increase in the utilization of the distributed generation in the structure of the energy hub [16]. To achieve an optimal plan for the energy hub, different modeling methods are scrutinized by considering the uncertainties. Moreover, various methods of modeling and optimizing the energy hub are evaluated, and the negative and positive specifications of the intended methods are presented [17]. In [18], load response is modeled as a strategy in the energy hub. In addition to the typical uncertainties, the uncertainty of energy carrier prices is tackled employing stochastic optimization. They concluded that the player's participation in the carbon market and inclusion of the demand response increase the flexibility level and decrease the operation cost by 2%. In [19], the comprehensive framework for resiliency in the electric power industry is discussed. This framework includes serious event modeling and tries to increase resiliency in different areas; following this, the use of MGs as a source of resiliency is investigated. Finally, mitigation strategies applied by MG operators that increase the resiliency level in the presence of severe outage events are assessed.

The resilience of water-electricity distribution systems against Hurricanes with multiple MGs using clean strategies is studied [20]. This reference investigates the main problem and two sub-problem issues to increase resiliency in systems against hurricanes. The MGs apply to increase resiliency to the water-electricity distributions system. The main problem is minimizing the investment cost while is considered resilience improvement strategies and the expected inaccessibility values of loads. This model is formulated based on stochastic programming. Also, clean energy includes upgrading the size of storage and line hardening in the electricity distribution system and water tanks in the water distribution system. The results demonstrate the effectiveness of the proposed method for improving resiliency. In [21] illustrate a framework for day-ahead market optimal charging of Electric Vehicles (EVs) is investigated. Optimizing active and reactive power exchange at any period could prevent the uncontrolled charging of these vehicles and enhance the profit of EV owners and network operators simultaneously.

Table 1
Comparison of this study with previous studies.

Refs.	Test system	Problem Type	Objective	Storages Loss	Storage	Load modeling	Resilience index	Convertor	Input data
[4]	Hub	MILP	Minimizing cost	×	✓	Normal	×	CHP, Trans, Boiler,EV,PV, WT	Electricity, Gas, Solar, Wind
[5]	Multi Energy Carrier microgrids	MIP	Maximizing resilience	×	✓	Critical, Non-Critical load	✓	Trans, CHP, Boiler,DG	Electricity, Gas
[6]	Hub	MIP	Minimizing cost	×	✓	Normal	×	CHP, Boiler,Trans, WT	Electricity, Gas, Wind
[8]	Microgrid	MILP	Minimizing (cost transactions +VOLL)	×	✓	Normal	✓	Trans, MT,WT, PV, EV	Electricity, Solar, Wind,
[9]	6-bus test system	MILP +semi integers	Minimizing (Cost+Emissions)	×	✓	Normal	×	Trans, WT, PHEV	Electricity,Wind
[10]	IEEE 33-bus electric system	LP	Minimizing cost	×	✓	Normal	✓	CHP, Boiler,Trans, Heat pump, PV, WT	Electricity, Solar, Wind, Gas
[11]	Hub	LP	Minimizing cost	×	✓	Normal	×	CHP, Boiler,Trans, absorption chillers, air conditioners	Electricity, Gas, Air
[12]	Hub	MINLP	Minimizing cost	×	✓	Normal	×	CHP, Boiler,Trans, CCHP,Heater	Electricity, Gas, Heat
[13]	Hubs	MINLP	Minimizing cost	×	✓	Normal	×	Trans, PtG, GfG, WT	Electricity, Gas, Solar, Wind
[14]	Modified IEEE 33-bu	LP	Maximizing accessibility of loads to power and water	×	✓	fixed, shiftable and curtailable loads	✓	Trans,DG, PV, WT	Electricity, Water, Wind, Solar
[16]	Hubs	MILP	Minimizing planning cost	×	✓	Normal	×	CHP, Boiler,Trans, WT,PV	Electricity, Gas, Heat
[18]	Hub	MILP	Minimizing cost	×	✓	Normal	×	CHP, Boiler,Trans, PtG, WT	Electricity, Gas, Wind
[20]	Modified IEEE 33-bu	LP	Minimizing (the expected inaccessibility values of loads+ investment cost)	×	✓	Critical, Non-Critical load	✓	Trans,DG, PV, WT	Electricity, Water, Wind, Solar
[21]	city of Kowloon and a IEEE 33 bus	MINLP	Minimizing costs of losses and charging EVs	×	✓	Normal	×	Trans,EVs	Electricity, Wind, Temperature
[27]	Multi Energy Hubs	NLP	Minimizing electrical and gas costs	×	✓	Normal	✓	Trans,CHP, Boiler, WT	Electricity, Gas, Heat, Wind
[28]	6-bus And IEEE RTS-79	LP	Maximizing resilience	×	✓	Normal	✓	Trans,CHP, Boiler, PtG, coal-fired, gas-fired	Electricity, Gas, Heat, Coal
[29]	IEEE 14-bus	MILP	Maximizing resilience	×	✓	Normal	✓	Trans, PtG, GtP	Electricity, Gas
[31]	Hub	MILP	Minimizing costs	✓	✓	Normal	×	CHP, Boiler,Trans, WT	Electricity, Gas, Wind
[32]	Distribution network	NLP	Maximizing Flexibility	×	✓	Normal	×	Trans,Boiler, PV, WT	Electricity, Gas, Wind, Solar
[33]	IEEE 6-bus and IEEE 24-bus	MILP	Minimizing costs	×	✓	Normal	×	CHP, Trans, WT,Boiler Hydrogen to power, Power to hydrogen	Electricity, Gas, wind
[35]	Microgrids	NLP	Minimizing cost	×	✓	Critical, Non-Critical load	✓	CHP, Boiler,Trans, PV,WT	Electricity, Gas, Wind, Solar
This paper	Hub	MINLP	Minimizing cost Maximizing Resiliency	✓	✓	Critical NC-S, NC-NS	✓	CHP, Boiler,Trans, CCHP,Heater	Electricity, Gas, Heat

Moreover, Considering the effective parameters on electrical energy consumption of EVs and their driving pattern, a proposed framework is used to develop a route mapping algorithm, which can provide better services to EV owners. Based on Kowloon's traffic data and geographic information, simulations were performed using an interior-point optimization method, and an IEEE 33 bus system was implemented. The results represent that integrating charging of EVs with a route mapping algorithm can decrease the loss costs of the network during the time of EVs' presence and the selling price of electricity to EV owners by 24.93% and 33.6%, respectively Compared to an uncontrolled state. In [22], the distribution systems containing MGs are described and the advantage compared to their shortcoming. Studying the level of distribution system resiliency against natural disasters discuses efficiently managing distributed generation (DGs).To do this, two different case studies (namely: moderate and severe damages) are assumed to establish various scenarios concerning different levels of failure.

The result of [23] shows that proper design enables the renewable energy and storage system integrated MGs to improve the resiliency of large building whiteout backup diesel generators (BDG). The [24] proposed evaluating the effect of the energy reliability indices on the economical parameters of CUPs in a restructuring environment using game theory. The intended indices such as energy not supplied are used to evaluate the impacts of reliability through the Monte-Carlo simulation. In [25], innovates offering strategy for combined heat and power systems concentrating solar power and compressed air energy storage that Virtual power plant (VPP) performs as a price-maker. The Karush–Kuhn–Tucker conditions are used in the optimization method. The mathematical model of this problem is implemented based on Mixed Integer Linear Programming (MILP). With the proposed method, the profit will rise by 2%, and the market price for electricity will increase by up to 6% compared to the system without compressed air energy storage.

Evaluation of flexibility in the power system based on the fragility curve and uncertainty when the server event occurs is Ref. [26]. The results are shown in the different intensities of events. The model system is IEEE 30 buses, simulated by considering 10,000 scenarios with various events in terms of position and intensity level on the power system. Moreover, Monte Carlo simulations are used to calculate resiliency criteria. Game theory is used in the problem of planning hub systems [27]. Considering the energy conversion in the energy hubs and the relationships between energy hubs, an optimal schedule for the mentioned model was determined based on game theory. In the proposed method, different wind speeds were investigated. The simulation results showed that the optimal planning method based on game theory has a higher resistance in multi-energy hub systems (MEHs) [28]. Proposed a coordinated operation using on regional-district for increasing resiliency in severe conditions. As well as, a bi-way flow model for the Integrated Energy System (IES) has been established based on power plant gas technologies. Gas and electricity network optimization is simultaneously done by regional IES, On the other hand, coordination between storage and converters is created by district IES. The results showed that the resiliency increased in the proposed model [29]. The addition of MGs in electricity and gas networks that are interdependent is investigated and its effect on resilience is expressed. In the intended network, graph and network theories have been used. Optimization results demonstrated that MGs can help improve overall resiliency. Because MGs can provide instant energy. In [30], details of resiliency modeling are presented in four dimensions: modeling goals and criteria, resiliency scenarios, control methods, and resiliency strategies. In resiliency scenarios, uncertainties are examined that include input data, probability status, DGs, and the relationship between power systems and other networks (such as gas networks). Moreover, dynamic control energy, optimal power flow, and management systems are the main approaches used to the resiliency model [31]. Studies the optimization of MECs in which wind farms are included as inputs and energy storage are used in the networks. In this case, the purpose is to provide electrical and thermal load. Stochastic programming is used in the problem. Uncertainties include the market prices and demand and wind speed. The results illustrate that the addition of a new source of thermal energy changes the optimal performance of the MECs, in conclusion, using the thermal energy market reduces operation costs by 4.8%.

A probabilistic nonlinear structure is proposed to maximize the flexibility considering power network constraints and EPs constraints using power flow in [32]. Hence, the proposed model should deliver improved voltage profiles, congestion reduction, robust thermal comfort during reserve calls, and efficient utilization of multi-energy storage. Using the proposed model, the multi-energy MG performance is sustainable, essential to modern smart cities. The proposed structure is used for a distribution network in the UK. Results show how equipment scheduling and demand response help observe electricity parameters constraints and maximize MEM flexibility.

The strategic scheduling of a multi-energy carrier system in the day-ahead market context based on bi-level optimization is investigated [33, 34]. Karush-Kuhn-Tucker (KKT) conditions are used for converting the bi-level nonlinear problem into a single-level MILP. A hybrid stochastic programming and robust optimization are applied for solving the problem [35]. Presents a new method that minimizes Networked Multi-Carrier Microgrid (NMCMG) costs related to the operation, CO2 emissions, maintenance, start-up and shutdown costs of units, and fines, incentives, and as reducing loads during unforeseen damages. In addition, the method examines time-based of demand response programs and investigates incentive-based of DRR.

1.3. Contribution

In this paper, an attempt is made to address the research gaps of the resiliency in hub energy. The main purpose of this paper is to increase the resilience of the energy hub, which should be done at the lowest cost. On the other hand, determining the critical loads in the energy hub is one of the issues that has been less studied in other papers. The operation of the energy hub should supply critical loads with the help of storage devices in the severe events. The share of critical and non-critical loads fed from the hub inputs is formulated in this paper. Also, the classification of non-critical loads is considered in both supplied and non-supplied ones. Considering storage losses is also one of the issues that are less discussed in other papers. Table 1 shows a general view of the previous papers and illustrates their defects. This paper deals with the optimal economical operation of the energy hub, which aims to minimize the feed cost of critical and non-critical loads (CNCLs) and the utilization cost of the storage device. At the same time, feeding the critical loads is the main priority of this approach for increasing resiliency. In other words, there is a challenge between increasing the resiliency of the critical loads and minimizing the total cost of the energy hub.

Innovations and contributions of this paper in comparison with the reviewed articles are as follows:

- In addition, to minimize the total cost of the energy hub, the proposed approach increases the resiliency of the critical loads.
- It determines the share of CNCLs fed by the energy hub's input carriers.
- In addition to the heating/cooling/electrical system efficiency, the losses attributed to the energy storage devices are also considered.
- Use a comprehensive scheme of energy hubs to increase the resiliency.
- classification of non-critical loads to supplied and non-supplied.

1.4. Organization

The different parts of this article are categorized as follows: The energy hub concept, resiliency modeling, economic dispatch of energy hub are described in the method part. The results include assumptions, a

Fig. 1. Energy hub input-output model.

case study, and a review of the simulation results. Finally, the general conclusion is explained in the last part.

For these purposes, the operation of the energy hub is formulated in GAMS software, and the DICOPT (DIscrete and Continuous OPTimizer) solver is used.

A relaxation strategy based on the outer-approximation algorithm is implemented in this solver procedure. Moreover, the main settings used in the DICOPT are as follows:

- Integer value tolerance is equal to 10^{-6}.
- Maximum number of cycles is equal to 20.
- Default number of iterations is 2×10^{4}.
- Default running time is 2000 s.
- Optimality tolerance is equal to 10^{-3}.

2. Method

2.1. Energy hub concept

The energy hub has several inputs, converters and storage elements, and several outputs, as shown in Fig. 1. furthermore, the relationship between inputs and outputs is specified in Eq. (1). Where *Pin* is the input, *Pout* is the output and *A* is the coupling matrix.

$$\begin{bmatrix} Pout-e \\ Pout-h \\ Pout-c \end{bmatrix} = \begin{bmatrix} A11 & A12 & A13 \\ A21 & A22 & A23 \\ A31 & A32 & A33 \end{bmatrix} \begin{bmatrix} Pin\_e \\ Pin\_g \\ Pin\_H \end{bmatrix} \quad (1)$$

The mentioned energy hub has three inputs and three outputs connected by a coupling matrix. Given that the relation between input and output is established by converters, and since the efficiency of the converters is less than 100%, so the values of the coupling matrix elements in each array are between zero and one, as shown in Eq. (2).

Since the output powers are obtained from the input power, the output powers are less than or equal to the input powers. In the other words, the sum of rows of the coupling matrix is less than or equal to one, which is expressed in Eq. (3):

$$0 \le A_{mn} \le 1 \; \forall \, m \in \{\hat{a} \; . \; \hat{b} \; ..... \; \hat{z}\} \; n \in \{a.b \; .....z\} \quad (2)$$

$$0 \le \sum_{n} A_{mn} \le 1 \quad (3)$$

A complete energy hub is shown more detail with storage elements and converters in Fig. 2.

Furthermore, the dispatch matrix is expressed based on the relation of the input carriers to the converters, which is shown in Eq. (4). For example, gas input enters to CHP, Boiler, and CCHP with percentages v1, v2, and (1-v1-v2) respectively. In order to supply the required loads and minimize costs, the amount of input and output power of CHP and CCHP is crucial factor to be considered (input-output model). Due to the scope of this paper, the dynamic model of CHP and CCHP is not the focus point of this paper and this issue is left to be fully addressed in our future research work.

$$\begin{bmatrix} P\_e \\ P\_chp \\ P\_cchp \\ P\_b \\ P\_H \end{bmatrix} = \begin{bmatrix} 1 & 0 & 0 \\ 0 & v1 & 0 \\ 0 & v2 & 0 \\ 0 & 1-v1-v2 & 0 \\ 0 & 0 & 1 \end{bmatrix} \begin{bmatrix} Pin\_e \\ Pin\_g \\ Pin\_H \end{bmatrix} \quad (4)$$

Eq.)5(shows the relationship between the output of the power hub and the converters and Eq. (6) represents the relation between output to each input.

$$\begin{matrix} Pout-e \\ \lceil Pout-h \rceil \\ Pout-c \end{matrix} = \begin{bmatrix} \eta_e & \eta\_chp_e & \eta\_cchp_e & 0 & 0 \\ 0 & \eta\_chp_h & \eta\_cchp_h & \eta_b & \eta_H \\ 0 & 0 & \eta\_cchp_c & 0 & 0 \end{bmatrix} \begin{bmatrix} P\_e \\ P\_chp \\ P\_cchp \\ P\_b \\ P\_H \end{bmatrix} \quad (5)$$

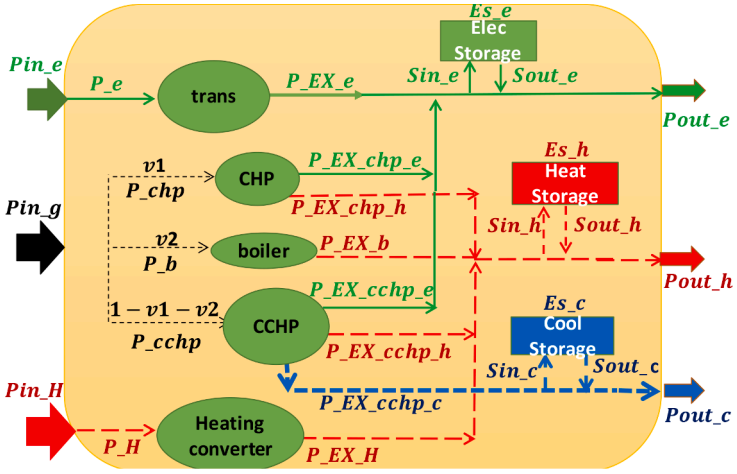

Fig. 2. Detailed view of an energy hub with storage and converters.

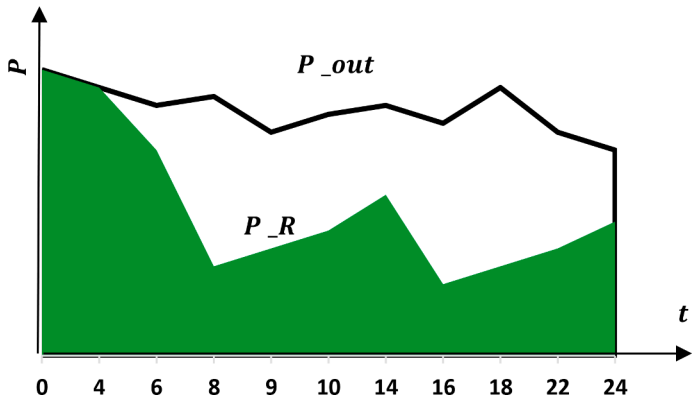

Fig. 3. Load condition associated with a severe event.

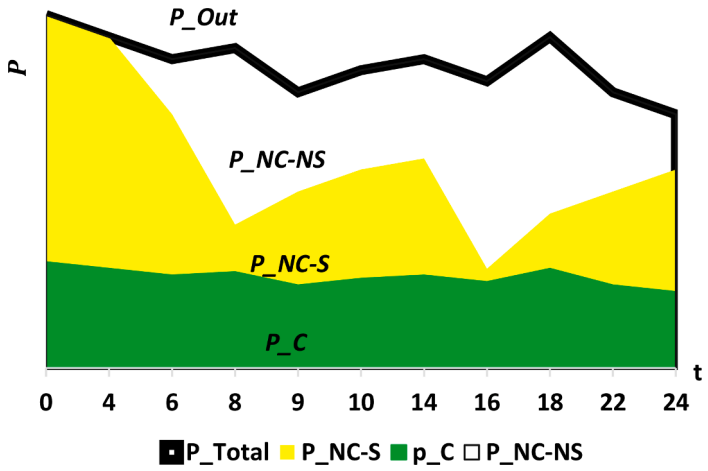

Fig. 4. The load categorization after a severe event.

$$\begin{matrix} Pout-e \\ \lceil Pout-h \rceil = \\ Pout-c \end{matrix} \begin{bmatrix} \eta_e & v1*\eta\_chp_e + v2*\eta\_cchp_e & 0 \\ 0 & v1*\eta\_chp_h + v2*\eta\_cchp_h + (1-v1-v2)*\eta_b & \eta_H \\ 0 & \eta\_cchp_c & 0 \end{bmatrix} \begin{bmatrix} Pin\_e \\ Pin\_g \\ Pin\_H \end{bmatrix} \tag{6}$$

Furthermore, storage units help the supply of load; considering storage units installed inside the energy hub, Eq. (6) turns into Eq. (7)

$$\begin{matrix} Pout-e \\ \lceil Pout-h \rceil = \\ Pout-c \end{matrix} \begin{bmatrix} \eta_e & v1*\eta.chp_e + v2*\eta.cchp_e & 0 \\ 0 & v1*\eta.chp_h + v2*\eta.cchp_h + (1-v1-v2)*\eta_b & \eta_H \\ 0 & \eta.cchp_c & 0 \end{bmatrix} \begin{bmatrix} Pin.e \\ Pin.g \\ Pin.H \end{bmatrix}$$
$$(Sout-e)-(Sin-e)$$
$$+\lceil (Sout-h)-(Sin-h) \rceil$$
$$(Sout-c)-(Sin-c) \tag{7}$$

2.2. Resiliency modeling

Resiliency is the ability to withstand severe events (low frequency and high impact) and restore restoration and recovery in the shortest interruption. Fig. 3 depicts the output load of the system at normal state and severe events state. The resiliency index R (t) is specified according to Eq. (8) that $P\_R\ (t)$ is the output load after the event and $P\_Out\ (t)$ is the output load of the system without event. Therefore, maximizing the mentioned index increases system resiliency during events.

$$\mathrm{R(T)} = \frac{\int_0^T P\_R(t)}{\int_0^T P\_Out(t)} \tag{8}$$

In this paper, the output loads are categorized into CNCLs, that non-critical loads themselves consist of two parts: non-critical loads that are fed (NC-S) after the event and non-critical loads that are not fed (NC-NS). The load categorization after severe event is illustrated in Fig. 4. Due to the importance of critical loads in the network, the main priority is to feed critical loads, and in the next step, non-critical loads must be fed. The R1 index is presented as the resiliency index in this paper according to Eq. (9). The mentioned index aims to increase the resiliency of the critical load.

$$\mathrm{R1(T)} = \frac{\int_0^T P\_c(t)}{\int_0^T P\_Out(t)} \tag{9}$$

2.3. Economic dispatch

The objective function is defined as Eq. (10), which minimizes the

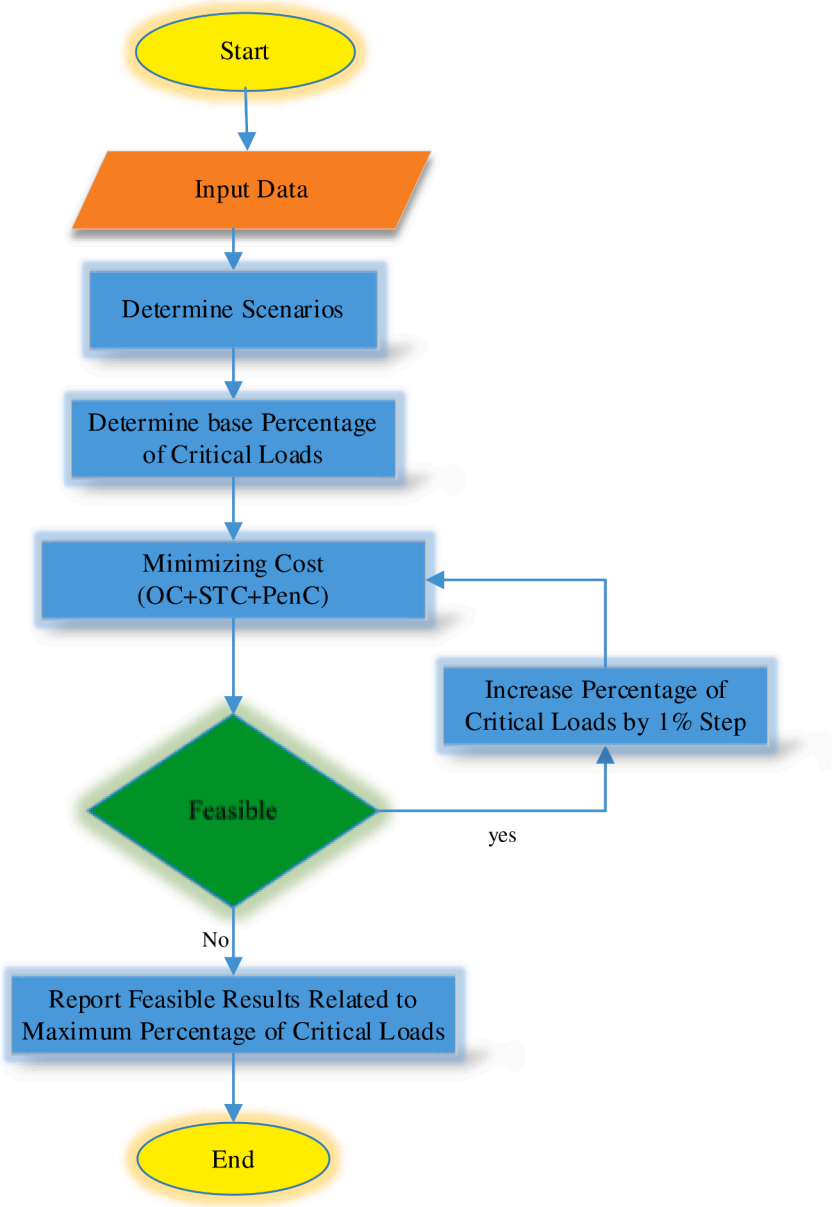

Fig. 5. Flowchart of optimization process.

Table 2
Technical characteristics of energy hub elements.

Hub Element	η_e	η_h	η_c	P_Max	P_Min	Sin-Min	Sin-Max	Sout-Min	Sout-Max	L_ESe	L_ESh	L_ESc
Heater(H)		0.92		6	0.1							
Trans(e)	0.97			30	0							
CHP	0.42	0.23		13	0.1							
CCHP	0.42	0.15	0.18	18	0.2							
Boiler(b)		0.78		4	0.1							
ES_e	0.95			20	0	0	5	0	5	0.01		
ES_h		0.94		10	0	0	5	0	5		0.03	
ES_c			0.93	3	0	0	1	0	1			0.04

total cost in a short-term operation problem over a 24 h horizon.

$$OF = minimizing\ (OC + STC + PenC) \tag{10}$$

The objective function (OF) consists of three parts. OC is the cost of feed to CNCLs (Operation Cost). The second term in Eq. (10) shows the usage costs of energy storage (STC). Penalty cost for the NC-NS load is expressed in the last term of Eq. (10).

Since the feed of critical loads is the main priority, the price of the input carriers (electricity, gas, heat) that feed the critical loads are multiplied by α in every period, the same interpretation is valid regarding non-critical load but since the latter is less important, the price of input carriers feeding non-critical loads is multiplied by β, which is

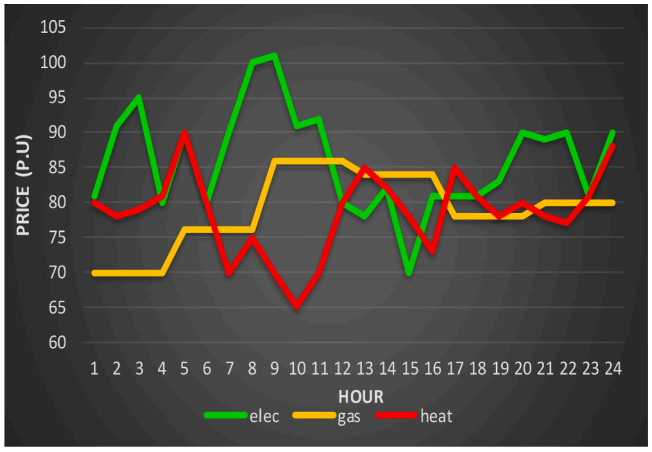

Fig. 6. Electricity/heat/gas prices.

less than α. Eqs. (11)–(27) represent the mentioned explanations.

$$OC = \sum_t (OC1_t + OC2_t + OC3_t + OC4_t + OC5_t + OC6_t + OC7_t + OC8_t + OC9_t + OC10_t + OC11_t + OC12_t + OC13_t + OC14_t + OC15_t + OC16_t) \tag{11}$$

That $OC1_t$ and $OC2_t$ in Eqs. (12) and (13) are the feeding costs of Critical and Non-critical electrical loads ($CNCL_e$), respectively, that are fed by input electric power of the transformer at t-hour.

$$OC1_t = \sum_j \frac{P\_e\_c_t}{P\_e\_c_t + P\_e\_ncs_t} \times \alpha \times P\_e_{j,t} \times \pi\_e_t \tag{12}$$

$$OC2_t = \sum_j \frac{P\_e\_ncs_t}{P\_e\_c_t + P\_e\_ncs_t} \times \beta \times P\_e_t \times \pi\_e_t \tag{13}$$

$OC3_t$ and $OC4_t$ in Eqs. (14) and (15) are the feeding costs of $CNCL_e$, respectively, that are fed by input gas of the CHP at t-hour.

$OC5_t$ and $OC6_t$ in Eqs. (16) and (17) are the feeding costs of critical and non-critical heating loads ($CNCL_h$), respectively, fed by input gas of the CHP at t-hour. It should be noted that to feed the $CNCL_e$ fed by CHP; it could be obtained by the ratio of CHP output electrical to the total output (heat and electricity) from CHP. In addition, to feed the $CNCL_h$ which CHP feeds could be obtained by the ratio of CHP output heat to the total output (electricity and heat) from CHP. The heat/electrical output of the CHP depends on their efficiencies.

$$OC3_t = \sum_j \frac{P\_e\_c_t}{P\_e\_c_t + P\_e\_ncs_t} \times P\_chp_{j,t} \times \pi\_g_t \times \alpha \times \frac{P\_Ex\_chp\_e_{j,t}}{P\_Ex\_chp\_e_{j,t} + P\_Ex\_chp\_h_{j,t}} \tag{14}$$

$$OC4_t = \sum_j \frac{P\_e\_ncs_t}{P\_e\_c_t + P\_e\_ncs_t} \times P\_chp_{j,t} \times \pi\_g_t \times \beta \times \frac{P\_Ex\_chp\_e_{j,t}}{P\_Ex\_chp\_e_{j,t} + P\_Ex\_chp\_h_{j,t}} \tag{15}$$

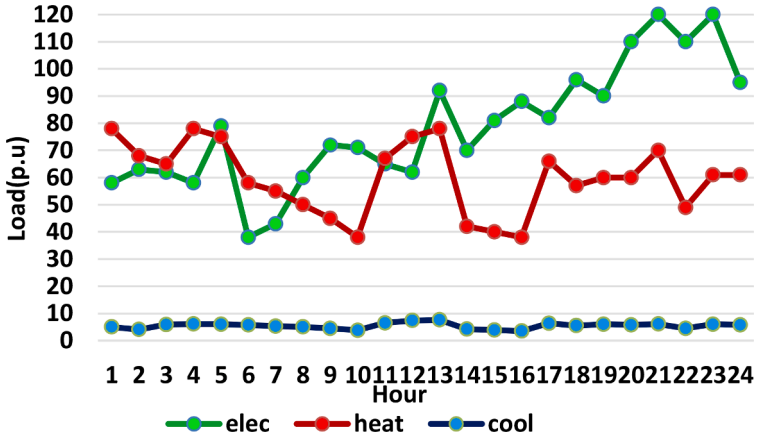

Fig. 7. Electrical, heating, and cooling loads.

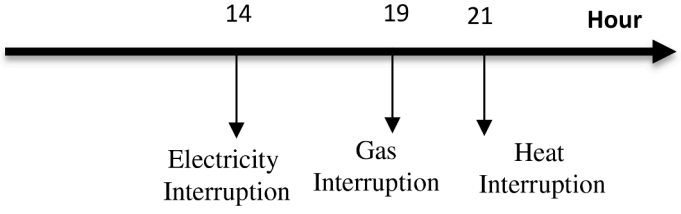

Fig. 8. Chronological events chain.

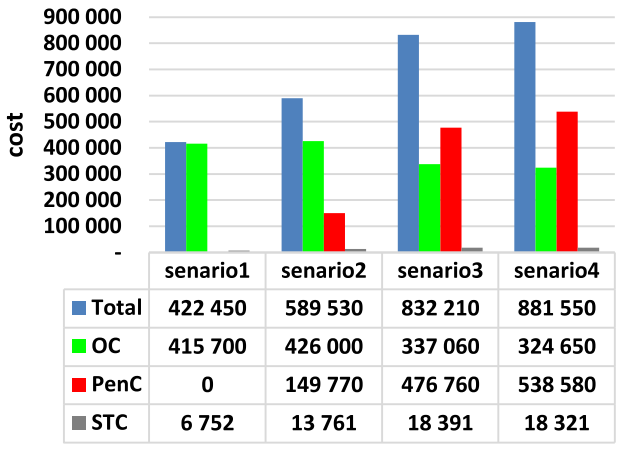

	senario1	senario2	senario3	senario4
Total	422 450	589 530	832 210	881 550
OC	415 700	426 000	337 060	324 650
PenC	0	149 770	476 760	538 580
STC	6 752	13 761	18 391	18 321

Fig. 9. The result of total cost in each scenario.

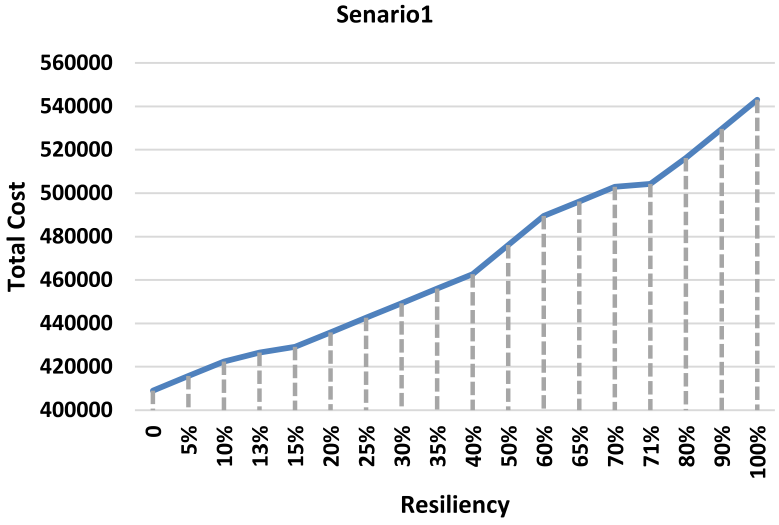

Fig. 10. The total cost based on resiliency index (R1) in scenario 1.

$$OC5_t = \sum_j \frac{P\_h\_c_t}{P\_h\_c_t + P\_h\_ncs_t} \times P\_chp_{j,t} \times \pi\_g_t \times \alpha \times \frac{P\_Ex\_chp\_h_{j,t}}{P\_Ex\_chp\_e_{j,t} + P\_Ex\_chp\_h_{j,t}} \tag{16}$$

$$OC6_t = \sum_j \frac{P\_h\_ncs_t}{P\_h\_c_t + P\_h\_ncs_t} \times P\_chp_{j,t} \times \pi\_g_t \times \beta \times \frac{P\_Ex\_chp\_h_{j,t}}{P\_Ex\_chp\_e_{j,t} + P\_Ex\_chp\_h_{j,t}} \tag{17}$$

$OC7_t$ and $OC8_t$ in Eqs. (18) and (19) are the feeding costs of $CNCL_h$, respectively, that are fed by the input gas of the Boiler at t-hour.

$$OC7_t = \sum_j \frac{P\_h\_c_t}{P\_h\_c_t + P\_h\_ncs_t} \times \alpha \times P\_b_{j,t} \times \pi\_g_t \tag{18}$$

$$OC8_t = \sum_j \frac{P\_h\_ncs_t}{P\_h\_c_t + P\_h\_ncs_t} \times \beta \times P\_b_{j,t} \times \pi\_g_t \tag{19}$$

$OC9_t$ and $OC10_t$ in Eqs. (20) and (21) are the feeding costs of CNCLe, respectively, that are fed by input gas of the CCHP at t-hour

$OC11_t$ and $OC12_t$ in Eqs. (22) and (23) are the feeding costs of $CNCL_h$, respectively, that are fed by input gas of the CCHP at t-hour.

$OC13_t$ and $OC14_t$ in Eqs. (24) and (25) are the feeding costs of critical and non-critical cooling loads ($CNCL_c$), respectively, that are fed by input gas of the CCHP at t-hour.

It should be noted that to feed the critical and non-critical electrical load fed by CCHP, it could be obtained by the ratio of CCHP output electrical to the total output (heat and electricity and cool) from CCHP. In addition, to feed the critical and non-critical heating load that CCHP feeds, it could be obtained by the ratio of CCHP output heat to the total output (.heat and electricity and cool) from CCHP. Moreover, to feed the critical and non-critical cooling load that CCHP feeds, could be obtained by the ratio of CCHP output cool to the total output (heat and electricity and cool) from CCHP.

The heat/electricity/cool output of the CCHP depends on their efficiencies.

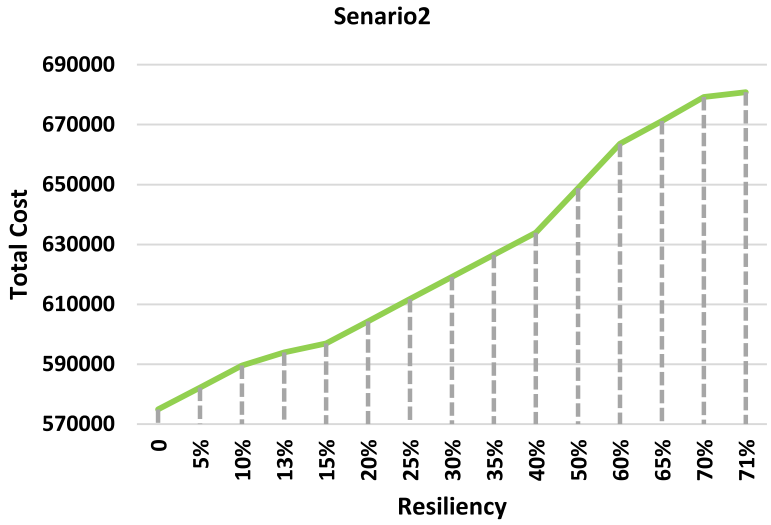

Fig. 11. The total cost based on resiliency index (R1) in scenario 2.

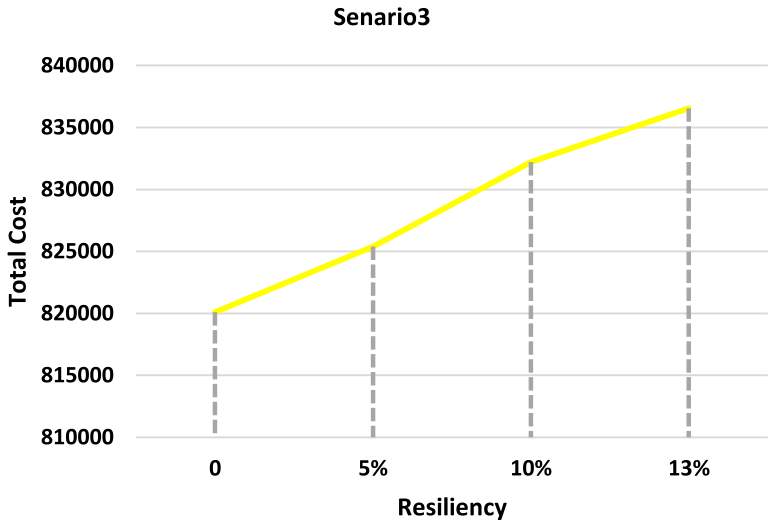

Fig. 12. The total cost based on resiliency index (R1) in scenario 3.

$$OC9_t = \sum_j \frac{P\_e\_c_t}{P\_e\_c_t + P\_e\_ncs_t} \times P\_cchp_{j,t} \times \pi\_g_t \times \alpha \times \frac{P\_Ex\_cchp\_e_{j,t}}{P\_Ex\_cchp\_e_{j,t} + P\_Ex\_cchp\_h_{j,t} + P\_Ex\_cchp\_c_{j,t}} \tag{20}$$

$$OC10_t = \sum_j \frac{P\_e\_ncs_t}{P\_e\_c_t + P\_e\_ncs_t} \times P\_cchp_{j,t} \times \pi\_g_t \times \beta \times \frac{P\_Ex\_cchp\_e_{j,t}}{P\_Ex\_cchp\_e_{j,t} + P\_Ex\_cchp\_h_{j,t} + P\_Ex\_cchp\_c_{j,t}} \tag{21}$$

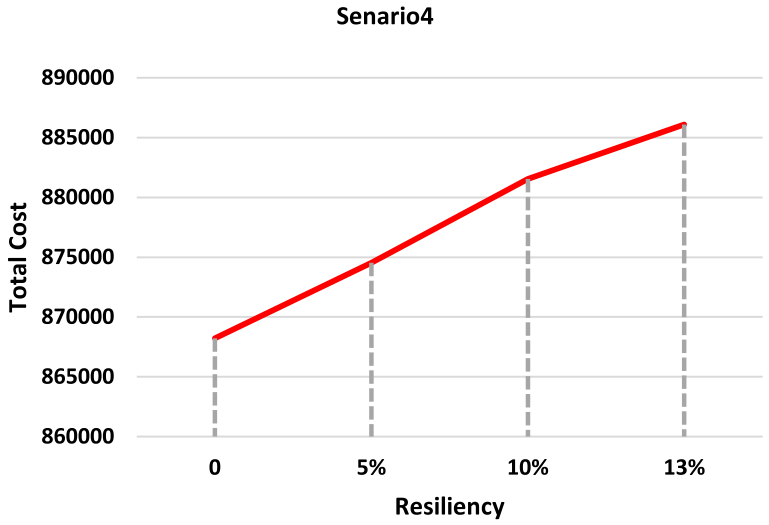

Fig. 13. The total cost based on resiliency index (R1) in scenario 4.

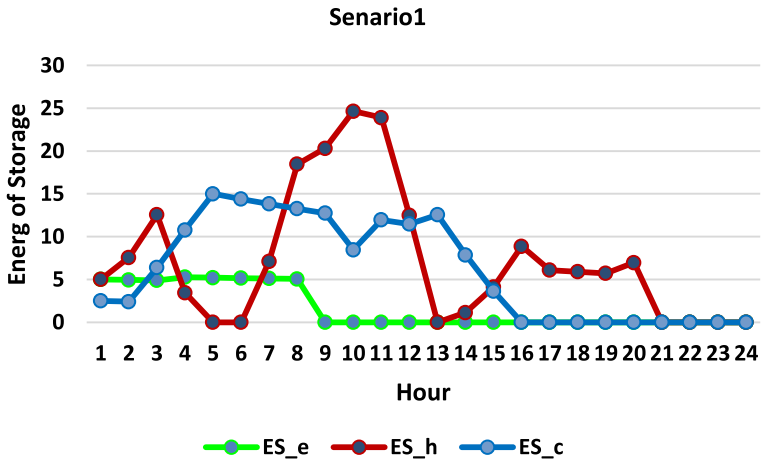

Fig. 14. The output energy of storages in scenario 1.

$$OC11_t = \sum_j \frac{P\_h\_c_t}{P\_h\_c_t + P\_h\_ncs_t} \times P\_cchp_{j,t} \times \pi\_g_t \times \alpha \times \frac{P\_Ex\_cchp\_h_{j,t}}{P\_Ex\_cchp\_e_{j,t} + P\_Ex\_cchp\_h_{j,t} + P\_Ex\_cchp\_c_{j,t}} \quad (22)$$

$$OC12_t = \sum_j \frac{P\_h\_ncs_t}{P\_h\_c_t + P\_h\_ncs_t} \times P\_cchp_{j,t} \times \pi\_g_t \times \beta \times \frac{P\_Ex\_cchp\_h_{j,t}}{P\_Ex\_cchp\_e_{j,t} + P\_Ex\_cchp\_h_{j,t} + P\_Ex\_cchp\_c_{j,t}} \quad (23)$$

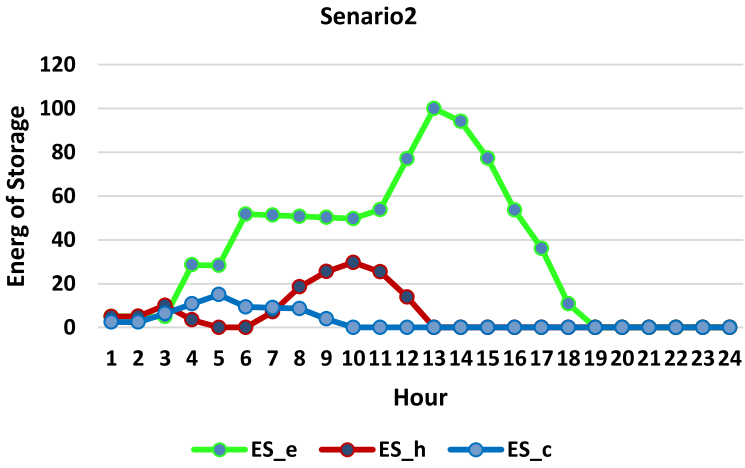

Fig. 15. The output energy of storages in scenario 2.

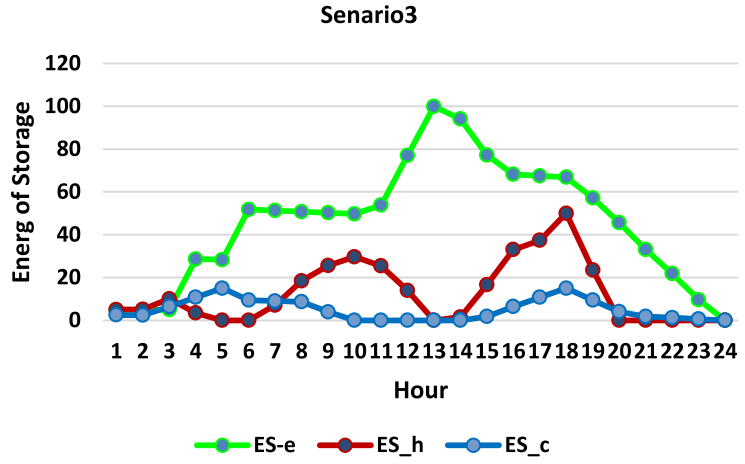

Fig. 16. The output energy of storages in scenario 3.

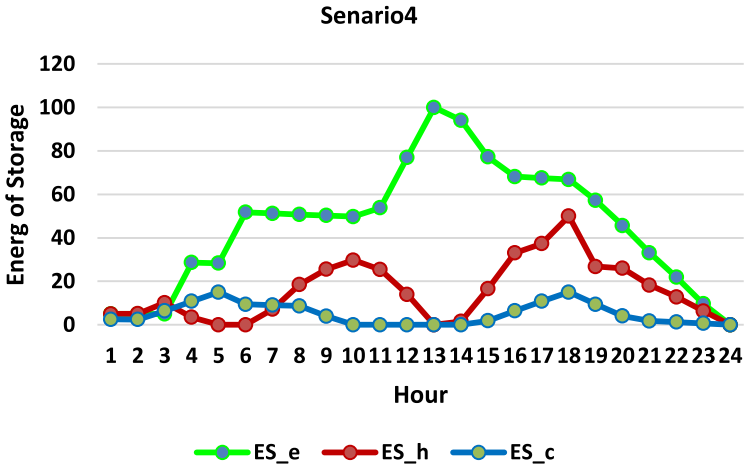

Fig. 17. The output energy of storages in scenario 4.

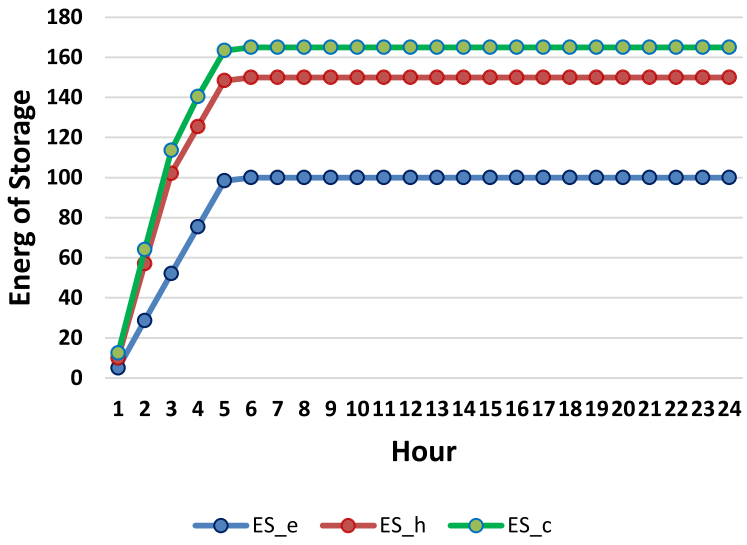

Fig. 18. The output energy of storages for introduced index [5] based on scenario 2.

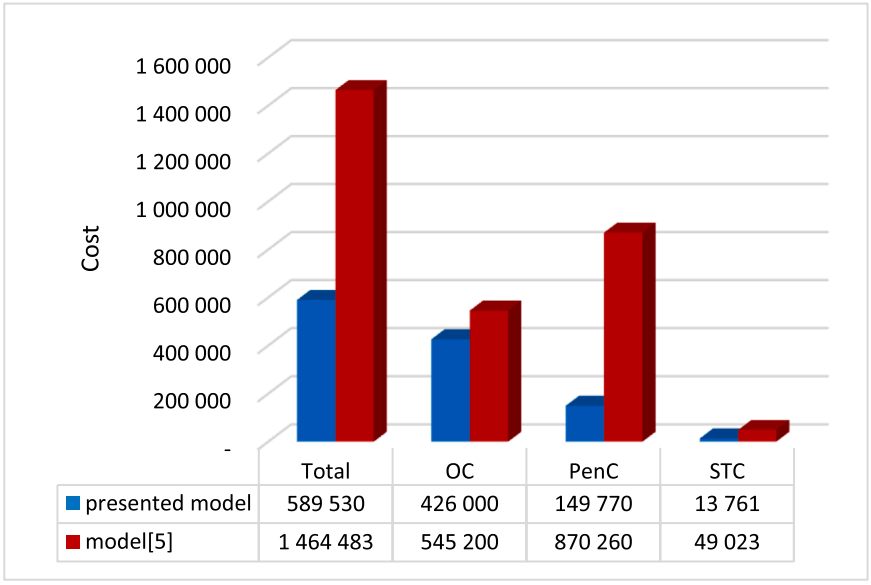

Fig. 19. A comparison results of [5] and presented method based on scenario 2.

$$OC13_t = \sum_j \frac{P\_c\_c_t}{P\_c\_c_t + P\_c\_ncs_t} \times P\_cchp_{j.t} \times \pi\_g_t \times \alpha \times \frac{P\_Ex\_cchp\_c_{j.t}}{P\_Ex\_cchp\_e_{j.t} + P\_Ex\_cchp\_h_{j.t} + P\_Ex\_cchp\_c_{j.t}} \tag{24}$$

$$OC14_t = \sum_j \frac{P\_c\_ncs_t}{P\_c\_c_t + P\_c\_ncs_t} \times P\_cchp_{j.t} \times \pi\_g_t \times \beta \times \frac{P\_Ex\_cchp\_c_{j.t}}{P\_Ex\_cchp\_e_{j.t} + P\_Ex\_cchp\_h_{j.t} + P\_Ex\_cchp\_c_{j.t}} \tag{25}$$

$OC15_t$ and $OC16_t$ in Eqs. (26) and (27) are the feeding costs of $CNCL_h$, respectively, that are fed by input heating of the Heater at t-hour.

$$OC15_t = \sum_j \frac{P\_h\_c_t}{P\_h\_c_t + P\_h\_ncs_t} \times \alpha \times P\_H_{j.t} \times \pi\_h_t \quad (26)$$

$$OC16_t = \sum_j \frac{P\_h\_ncs_t}{P\_h\_c_t + P\_h\_ncs_t} \times \beta \times P\_H_{j.t} \times \pi\_h_t \quad (27)$$

STC in Eq. (10) of the objective function is the usage costs of energy storage, obtained by multiplying the price of storage devices and the summation input/output power of storage devices per hour represented in Eq. (28).

$$STC = \sum_j \sum_t \pi\_Es\_e_{j.t}\left(Sin\_e_{j.t} + Sout\_e_{j.t}\right) + \sum_j \sum_t \pi\_Es\_h_{j.t}\left(Sin\_h_{j.t} + Sout\_h_{j.t}\right) + \sum_j \sum_t \pi\_Es\_c_{j.t}\left(Sin\_c_{j.t} + Sout\_c_{j.t}\right) \quad (28)$$

On the other hand, PenC in Eq. (10) of the objective function is penalty cost for the NC-NS load. Obviously, since the goal is to maximize the amount of CNCLs, the PenC item should be minimized. The calculation method is demonstrated in Eq. (29) which is obtained by multiplying the NC-NS load and the penalty factor considered for different types of load.

$$PenC = \sum_t P\_e\_ncns_t \times Pen\_e_t + \sum_t P\_h\_ncns_t \times Pen\_h_t + \sum_t P\_c\_ncns_t \times Pen\_c_t \quad (29)$$

The constraints are introduced in this paper as follows:

- The input electrical is equal to the sum of the input electrical of transformers according to Eq. (30)

$$Pin\_e_t = \sum_j P\_e_{j.t} \quad (30)$$

- The input gas is equal to the sum of the input gas of CHPs/CCHPs/Boilers according to Eq. (31)

$$Pin\_g_t = \sum_j P\_chp_{j.t} + \sum_j P\_cchp_{j.t} + \sum_j P\_b_{j.t} \quad (31)$$

- The input heat is equal to the sum of the input heat of Heaters according to Eq. (32)

$$Pin\_H_t = \sum_j P\_H_{j.t} \quad (32)$$

- The input power to each converter per hour should be fallen within the minimum and maximum power of a single convertor. Eqs. (33)–(37) illustrate this point

$$I\_e_{j.t} \times P\_e_j^{min} \le P\_e_{j.t} \le I\_e_{j.t} \times P\_e_j^{max} \quad (33)$$

$$I\_H_{j.t} \times P\_H_j^{min} \le P\_H_{j.t} \le I\_H_{j.t} \times P\_H_j^{max} \quad (34)$$

$$I\_chp_{j.t} \times P\_chp_j^{min} \le P\_chp_{j.t} \le I\_chp_{j.t} \times P\_chp_j^{max} \quad (35)$$

$$I\_cchp_{j.t} \times P\_cchp_j^{min} \le P\_cchp_{j.t} \le I\_cchp_{j.t} \times P\_cchp_j^{max} \quad (36)$$

$$I\_b_{j.t} \times P\_b_j^{min} \le P\_b_{j.t} \le I\_b_{j.t} \times P\_b_j^{max} \quad (37)$$

On the other side, the output of each converter depends on the efficiency of the equipment, and Ex represents the output of the converter.

CHP output power includes heating, and electricity and CCHP output power includes heating, cooling, and electricity. Eqs. (38)–(45) show the output limitations of the converter.

$$P\_Ex\_e_{j.t} = P\_e_{j.t} \times \eta\_e_j \quad (38)$$

$$P\_Ex\_chp\_e_{j.t} = P\_chp_{j.t} \times \eta\_chp\_e_j \quad (39)$$

$$P\_Ex\_chp\_h_{j.t} = P\_chp_{j.t} \times \eta\_chp\_h_j \quad (40)$$

$$P\_Ex\_cchp\_e_{j.t} = P\_cchp_{j.t} \times \eta\_cchp\_e_j \quad (41)$$

$$P\_Ex\_cchp\_h_{j.t} = P\_cchp_{j.t} \times \eta\_cchp\_h_j \quad (42)$$

$$P\_Ex\_cchp\_c_{j.t} = P\_cchp_{j.t} \times \eta\_cchp\_c_j \quad (43)$$

$$P\_Ex\_b_{j.t} = P\_b_{j.t} \times \eta\_b_j \quad (44)$$

$$P\_Ex\_H_{j.t} = P\_H_{j.t} \times \eta\_H_j \quad (45)$$

The inputs/outputs power in/from the storage per hour should be fallen within a single storage device's minimum and maximum power. Also, total capacity storage has a specific amount. Eqs. (46)–(54) show this point.

$$I\_ES\_e_{j.t} \times ES\_e_j^{min} \le ES\_e_{j.t} \le I\_ES\_e_{j.t} \times ES\_e_j^{man} \quad (46)$$

$$I\_ES\_e_{j.t} \times Sin\_e_j^{min} \le Sin\_e_{j.t} \le I\_ES\_e_{j.t} \times Sin\_e_j^{man} \quad (47)$$

$$I\_ES\_e_{j.t} \times Sout\_e_j^{min} \le Sout\_e_{j.t} \le I\_ES\_e_{j.t} \times Sout\_e_j^{man} \quad (48)$$

$$I\_ES\_h_{j.t} \times ES\_h_j^{min} \le ES\_h_{j.t} \le I\_ES\_h_{j.t} \times ES\_h_j^{man} \quad (49)$$

$$I\_ES\_h_{j.t} \times Sin\_h_j^{min} \le Sin\_h_{j.t} \le I\_ES\_h_{j.t} \times Sin\_h_j^{man} \quad (50)$$

$$I\_ES\_h_{j.t} \times Sout\_h_j^{min} \le Sout\_\ h_{j.t}\ \le\ I\_ES\_\ h_{j.t} \times Sout\_h_j^{man} \quad (51)$$

$$I\_ES\_c_{j.t} \times ES\_c_j^{min} \le ES\_c_{j.t} \le I\_ES\_c_{j.t} \times ES\_c_j^{man} \quad (52)$$

$$I\_ES\_c_{j.t} \times Sin\_c_j^{min} \le Sin\_c_{j.t} \le I\_ES\_c_{j.t} \times Sin\_c_j^{man} \quad (53)$$

$$I\_ES\_c_{j.t} \times Sout\_c_j^{min} \le Sout\_c_{j.t} \le I\_ES\_c_{j.t} \times Sout\_c_j^{man} \quad (54)$$

The power balance for various storages units is represented by Eqs. (55)–(57). It is worthy to note that two kinds of losses are conceivable in storage units:

1- the loss associated with the storage charging/discharging process, which is represented in storage units efficiency
2- Energy waste resulted from heating/colling/ electricity system internal losses, which depends on time. As time passes, more energy will be lost due to this characteristic of storage units

$$ES\_e_{j.t} = \left(\eta\_Se \times Sin\_e_{j.t}\right) - Sout\_e_{j.t} + ES\_e_{j.t-1}(1 - L\_ESe) \quad (55)$$

$$ES\_h_{j.t} = \left(\eta\_Sh\ \times Sin\_h_{j.t}\right) - Sout\_h_{j.t} + ES\_h_{j.t-1}(1 - L\_ESh) \quad (56)$$

$$ES\_c_{j.t} = \left(\eta\_Sc \times Sin\_c_{j.t}\right) - Sout\_c_{j.t} + ES\_c_{j.t-1}(1 - L\_ESc) \quad (57)$$

The power balance for various loads (electricity/cooling/heating) is represented by Eqs. (58)–(60).

$$P\_e\_c_t + P\_e\_ncs_t = \sum_j \left(P\_Ex\_e_{j.t} + P\_Ex\_chp\_e_{j.t} + P\_Ex\_cchp\_e_{j.t} + Sout\_e_{j.t} - Sin\_e_{j.t}\right) \quad (58)$$

$$P\_h\_c_t + P\_h\_ncs_t = \sum_j \left(P\_Ex\_H_{j.t} + P\_Ex\_b_{j.t} + P\_Ex\_chp\_h_{j.t} + P\_Ex\_cchp\_h_{j.t} + Sout\_h_{j.t} - Sin\_h_{j.t}\right) \quad (59)$$

$$P\_c\_c_t + P\_c\_ncs_t = \sum_j \left(P\_Ex\_cchp\_c_{j.t} + Sout\_c_{j.t} - Sin\_c_{j.t}\right) \quad (60)$$

On the other hand, the balance must be permanently established for output electric/heat/cool load. Eqs. (61)–(63) show this issue.

$$P\_e\_c_t + P\_e\_ncs_t + \ P\_e\_ncns_t = Pout\_e_t \quad (61)$$

$$P\_h\_c_t + P\_h\_ncs_t + \ P\_h\_ncns_t = Pout\_h_t \quad (62)$$

$$P\_c\_c_t + P\_c\_ncs_t + \ P\_c\_ncns_t = Pout\_c_t \quad (63)$$

In general, Fig. 5 shows the implementation and flowchart of the optimization process.

3. Results

3.1. Assumptions/case study

The test system is based on a comprehensive energy hub whose inputs include electricity/gas /heat and is connected to the input. The output contains loads (electricity /heat / cooling) fed by input carriers. The value of energy is assumed in P U, and the base amount is equal to 1MW. Moreover, prices are expressed in $ / MWh.

The price of charging/discharging electrical storage is equal to ($ 40) / MWh, and the price of charging/discharging heating storage is equal to ($ 35) / MWh, and the price of charging/discharging cooling storage is equal to ($ 36) / MWh.

The price coefficient for feeding the critical loads is equal to 1.6= α

The price coefficient for feeding the non-critical loads is equal to 1.2= β

The initial amounts of the electrical, heating, and cooling storage are equal to 1 Wh, 1 MWh, and 0.5 MWh, respectively.

Table 2 shows the technical characteristics of the intended energy hub elements. Here, the parameters of used model is identical to those of in [12,18,31].

(Heater (H), (trans), (CHP), (CCHP), Boiler (b), electrical .storage (ES_e), heat .storage (ES_h) and cool .storage (ES_c)). In addition, the penalty factors for not supplying a load of electrical, heating, and cooling are $ 600 / MWh, $ 550 / MWh, $ 480 / MWh, respectively. The critical load for all types of loads (electrical, heating, cooling) is considered 10% of the total load, supplied by the storage and input energies. Fig. 6 illustrates electricity, gas, and heat price offer. Fig. 7 shows the load curve of electricity/ heat/ cool. Data of [12,18,31] is used.

Fig. 8 shows the mentioned optimization problem investigated based on chronological events chain.

Therefore, the problem is examined in the following scenarios:

- Senario1: Electrical input ✓, Gas input ✓, Heat input ✓
- Senario2: Electrical input ×, Gas input ✓, Heat input ✓
- Senario3: Electrical input ×, Gas input ×, Heat input ✓
- Senario4: Electrical input ×, Gas input ×, Heat input ×

3.2. Simulation results

The total cost includes the cost of supply to CNCLs (OC), the cost of using storage devices (STC), and the penalty cost of NC-NS loads (PenC). Fig. 9 shows the total cost separately.

In all scenarios, the percentage of a critical load is at least 10% of the total load, which the energy hub must supply.

The result of scenarios shows that the total cost of energy hub has an increasing trend. Given that each scenario has a more severe event than the previous scenario, this trend seems logical. Nothing happened in the first scenario, so all the charges are met and the cost of the NC-NS penalty is zero. In the second scenario, when the electrical input is interrupted, less electrical load is supplied. However, due to the presence of CHP and CCHP, fed from the gas input, some of the output electrical load is supplied. In the third and fourth scenarios, the penalty cost of NC-NS load is a high percentage of the total cost. This issue is related to a lack of input resources and increases the cost of NC-NS load.

Under normal circumstances, the total cost is equal to $422,450, and in the case of a worst-case scenario, the cost is equal to $881,550. In the

worst-case scenario, $ 583,580 was paid as a penalty for NC-NS load, a 108% increase over normal.

Moreover, in various scenarios, the total cost for different percentages of critical loads is shown in Figs. 10–13.

The results show that in the first scenario, all the inputs are online; up to 100% of the total load could be considered the critical load. Considering the whole range of 0% to 100% causes a 33% increase in total cost, namely 134,060 $

Also, for an increase of 1% of the critical load in the energy hub, the average cost of the whole system increases by 1340 $.

In the second scenario, due to the interruption of electrical input, only up to 71% of the total load could be considered the critical load. Considering the whole range of 0% to 71% causes an 18% increase in total cost, namely 106,020 $

Moreover, for an increase of 1% of the critical load in the energy hub, the average cost of the whole system increases by 1493 $.

In the third scenario, due to electrical and gas outages, only up to 13% of the total load could be considered the critical load. Considering the whole range of 0–13 causes a 2% increase in total cost, namely 16,430 $

Also, for an increase of 1% of the critical load in the energy hub, the average cost of the whole system increases by 1260 $.

In the fourth scenario, due to the interruption of all inputs (electricity, gas, and heat), only 13% of the total load could be considered the critical load. Considering the whole range of 0–13% causes a 2% increase in total cost, namely 17,890 $.

Furthermore, for an increase of 1% of the critical load in the energy hub, the average cost of the whole system increases by 1376 $.

Furthermore, in Figs. 14–17, the storage device use for different scenarios is depicted.

As shown in Fig. 14 in the first scenario, due to the high price of electricity in $t = 8$ and $t = 9$, the electrical storage device is discharged during these hours. similarly, having said that the lowest price of the input heat is offered at $t = 9$ to $t = 11$, the highest charge of the heating storage is done during these hours. Moreover, For the cooling storage, due to the low gas price in $t = 1$ to $t = 4$, most storage is done during these hours.

Also, the electrical/heating /cooling storage percentage is 11%, 41%, and 48%, respectively.

In the second scenario in Fig. 15, due to the interrupt of input electrical at $t = 14$, the maximum amount of electrical storage occurs at $t = 13$ to compensate for the lack of electrical load, which is an obvious trend.

Moreover, the electrical/heating /cooling storage percentage is 80%, 14%, and 6%, respectively.

In the third scenario in Fig. 16, due to the interrupt of input electrical at $t = 14$ and the interrupt of input gas at $t = 19$, to compensate for the lack of electrical and heating loads, the maximum amount of electrical storage occurs at $t = 13$; furthermore, the maximum amount of heating storage also occurs at=18.

Furthermore, the electrical/heating /cooling storage percentage is 72%, 20%, and 8%, respectively.

In the fourth scenario in Fig. 17, similar to the third scenario, due to the interrupt of input electrical at $t = 14$ and the gas at $t = 19$, the maximum amount of electrical storage and heating is at $t = 13$ and $t = 18$, respectively, and afterward, interruption of CCHP gas input at $t = 18$ is the maximum cooling reserve at the same time. Also, the electrical/heating /cooling storage percentage is 69%, 23%, and 8%, respectively.

It is notable; the proposed model is not specific to any particular system and can be used for any system because critical loads such as hospitals, sensitive military areas, power plants, refineries, etc. are important in any system.

Critical loads are supplied using storage devices in this framework. Finally, the proposed model is compared with the one introduced in [5]. In both models, second scenario is used and the critical load is considered 10%. Fig. 18 shows the amounts of Energy stored based on the index presented in [5]. A comparison of total costs in both models is shown in Fig. 19. As a result, in [5], the amount of storage is 189% higher, but the overall cost has increased by 148%, which is caused by the lack of an economic approach. It is worth noting that both models can supply critical loads. Therefore, dealing with load supply with an economic approach is one of the important issues that is considered in the operation of the energy hub.

4. Conclusions

As mentioned, the energy system's resilience has been given special attention by planners and operators. Still, the issue of resilience has been less addressed from an economic point of view.

On the other hand, in severe cases due to system outages, load supply is of particular importance. Classification of energy hub loads is one of the important issues addressed. In this study, network loads were divided into two categories: critical loads and non-critical loads. Also, according to this classification, the issue of resilience was examined with an economic approach.

In this paper, the Optimization Problem based on Mixed Integer Linear Programming (MILP) was implement. In the problem structure, four scenarios were examined and each scenario has more severe events than the previous scenario. The trade-off between increasing critical load resiliency and reducing total costs was investigated. Determining the share of critical and non-critical loads supplied by input carriers was formulated. Studying the trend of total costs to increase the resilience of critical loads against severe events is one of the most important goals of this research.

The point-by-point finding of this paper are briefed as follows:

1 The findings showed that with increasing critical load resilience, total costs increase.
2 Moreover, in different scenarios, the use of storage devices helps to increase resiliency Furthermore, in severe events, using storage devices has an increasing trend, and.
3 The simulation proved that the maximum amount of storage is used in the presence of low prices for incoming energy carriers.

In future research, we will scrutinize the uncertainty of events occurring in various scenarios. Furthermore, capacity storage can be considered variable and optimum sizing of capacity storage in hub energy will be achieved.

CRediT authorship contribution statement

Jafar Khayatzadeh: Conceptualization, Methodology, Software. **Soodabeh Soleymani:** Supervision, Formal analysis. **Seyed Babak Mozafari:** Writing – original draft, Investigation. **Hosein Mohammadnezhad Shourkaei:** Writing – review & editing.

Declaration of Competing Interest

The authors have declared no conflict of interest.

References

[1] M.A. Mirzaei, M.Z. Oskouei, B. Mohammadi-Ivatloo, A. Loni, K. Zare, M. Marzband, et al., Integrated energy hub system based on power-to-gas and compressed air energy storage technologies in the presence of multiple shiftable loads, IET Gener. Trans. Distrib. 14 (13) (2020) 2510–2519.
[2] M. Papic, S. Ekisheva, E. Cotilla-Sanchez, A risk-based approach to assess the operational resilience of transmission grids, Appl. Sci. 10 (14) (2020) 4761.
[3] F.H. Jufri, V. Widiputra, J. Jung, State-of-the-art review on power grid resilience to extreme weather events: definitions, frameworks, quantitative assessment methodologies, and enhancement strategies, Appl. Energy 239 (2019) 1049–1065.
[4] X. Lu, Z. Liu, L. Ma, L. Wang, K. Zhou, N Feng, A robust optimization approach for optimal load dispatch of community energy hub, Appl. Energy 259 (2020), 114195.

[5] M.H. Amirioun, F. Aminifar, M. Shahidehpour, Resilience-promoting proactive scheduling against hurricanes in multiple energy carrier microgrids, IEEE Trans. Power Syst. 34 (3) (2018) 2160–2168.
[6] S.M. Ezzati, F. Faghihi, H.M. Shourkaei, S.B. Mozafari, S. Soleymani, Optimum operation of multi-energy carriers in the context of an energy hub considering a wind generator based on linear programming, J. Renew. Sustain. Energy 10 (1) (2018), 014702.
[7] M. Nazemi, M. Moeini-Aghtaie, M. Fotuhi-Firuzabad, P. Dehghanian, Energy storage planning for enhanced resilience of power distribution networks against earthquakes, IEEE Trans. Sustain. Energy 11 (2) (2019) 795–806.
[8] J. Najafi, A. Anvari-Moghaddam, M. Mehrzadi, C.L. Su, An Efficient Framework for Improving Microgrid Resilience Against Islanding With Battery Swapping Stations, IEEE Access 9 (2021) 40008–40018.
[9] S. Zeynali, N. Nasiri, M. Marzband, S.N. Ravadanegh, A hybrid robust-stochastic framework for strategic scheduling of integrated wind farm and plug-in hybrid electric vehicle fleets, Appl. Energy 300 (2021), 117432.
[10] M. Bao, Y. Ding, M. Sang, D. Li, C. Shao, J. Yan, Modeling and evaluating nodal resilience of multi-energy systems under windstorms, Appl. Energy 270 (2020), 115136.
[11] V. Thang, Y. Zhang, T. Ha, S. Liu, Optimal operation of energy hub in competitive electricity market considering uncertainties, Int. J. Energy Environ. Eng. 9 (3) (2018) 351–362.
[12] S.M. Ezzati, F. Faghihi, H. Mohammadnezhad Shourkaei, S.B. Mozafari, S Soleymani, Reliability assessment for economic dispatch problem in the energy hub concept, Energy Sources Part B Econ. Plan. Policy 13 (9–10) (2018) 414–428.
[13] H. Khani, A. Sawas, H.E. Farag, An estimation–based optimal scheduling model for settable renewable penetration level in energy hubs, Electr. Power Syst. Res. 196 (2021), 107230.
[14] J. Najafi, A. Peiravi, A. Anvari-Moghaddam, J.M. Guerrero, An efficient interactive framework for improving resilience of power-water distribution systems with multiple privately-owned microgrids, Int. J. Electr. Power Energy Syst. 116 (2020), 105550.
[15] S. Ranjbar, A.S. Al-Sumaiti, R. Sangrody, Y.J. Byon, M. Marzband, Dynamic clustering-based model reduction scheme for damping control of large power systems using series compensators from wide area signals, Int. J. Electr. Power Energy Syst. 131 (2021), 107082.
[16] S. Hemmati, S. Ghaderi, M. Ghazizadeh, Sustainable energy hub design under uncertainty using Benders decomposition method, Energy 143 (2018) 1029–1047.
[17] M. Mohammadi, Y. Noorollahi, B. Mohammadi-ivatloo, H. Yousefi, S Jalilinasrabady, Optimal scheduling of energy hubs in the presence of uncertainty-a review, J. Energy Manag. Technol. 1 (1) (2017) 1–17.
[18] R. Ghaffarpour, Stochastic optimization of operation of power to gas included energy hub considering carbon trading, demand response and district heating market, J. Energy Manag. Technol. 4 (3) (2020) 7–14.
[19] A. Hussain, V.H. Bui, H.M. Kim, Microgrids as a resilience resource and strategies used by microgrids for enhancing resilience, Appl. Energy 240 (2019) 56–72.
[20] J. Najafi, A. Peiravi, A. Anvari-Moghaddam, J.M. Guerrero, Resilience improvement planning of power-water distribution systems with multiple microgrids against hurricanes using clean strategies, J. Clean. Prod. 223 (2019) 109–126.
[21] A. Shahkamrani, H. Askarian-Abyaneh, H. Nafisi, M. Marzband, A framework for day-ahead optimal charging scheduling of electric vehicles providing route mapping: kowloon case study, J. Clean. Prod. 307 (2021), 127297.
[22] E. Galvan, P. Mandal, Y. Sang, Networked microgrids with roof-top solar PV and battery energy storage to improve distribution grids resilience to natural disasters, Int. J. Electr. Power Energy Syst. 123 (2020), 106239.
[23] E. Rosales-Asensio, M. de Simón-Martín, D. Borge-Diez, J.J. Blanes-Peiró, A Colmenar-Santos, Microgrids with energy storage systems as a means to increase power resilience: an application to office buildings, Energy 172 (2019) 1005–1015.
[24] M. Manbachi, M.R. Haghifam, The economical feasibility of combined heat and power systems in energy markets based on reliability, using dynamic game theory, Energy Sources Part B Econ. Plan. Policy 10 (1) (2015) 82–90.
[25] S. Sun, S.M. Kazemi-Razi, L.G. Kaigutha, M. Marzband, H. Nafisi, A.S. Al-Sumaiti, Day-ahead offering strategy in the market for concentrating solar power considering thermoelectric decoupling by a compressed air energy storage, Appl. Energy 305 (2022), 117804.
[26] A. Younesi, H. Shayeghi, A. Safari, P. Siano, Assessing the resilience of multi microgrid based widespread power systems against natural disasters using Monte Carlo Simulation, Energy 207 (2020), 118220.
[27] Y. Huang, W. Zhang, K. Yang, W. Hou, Y Huang, An optimal scheduling method for multi-energy hub systems using game theory, Energies 12 (12) (2019) 2270.
[28] M. Yan, Y. He, M. Shahidehpour, X. Ai, Z. Li, J Wen, Coordinated regional-district operation of integrated energy systems for resilience enhancement in natural disasters, IEEE Trans. Smart Grid 10 (5) (2018) 4881–4892.
[29] N. Yodo, T. Arfin, A resilience assessment of an interdependent multi-energy system with microgrids, Sustain. Resil. Infrastruct. 6 (1–2) (2021) 42–55.
[30] Y. Wang, A.O. Rousis, G. Strbac, On microgrids and resilience: a comprehensive review on modeling and operational strategies, Renew. Sustain. Energy Rev. 134 (2020), 110313.
[31] M. Vahid-Pakdel, S. Nojavan, B. Mohammadi-Ivatloo, K. Zare, Stochastic optimization of energy hub operation with consideration of thermal energy market and demand response, Energy Convers. Manage. 145 (2017) 117–128.
[32] S.M. Kazemi-Razi, H.A. Abyaneh, H. Nafisi, Z. Ali, M. Marzband, Enhancement of flexibility in multi-energy microgrids considering voltage and congestion improvement: robust thermal comfort against reserve calls, Sustain. Cities Soc. 74 (2021), 103160.
[33] N. Nasiri, S. Zeynali, S.N. Ravadanegh, M. Marzband, A hybrid robust-stochastic approach for strategic scheduling of a multi-energy system as a price-maker player in day-ahead wholesale market, Energy 235 (2021), 121398.
[34] H. Gharibpour, F. Aminifar, I. Rahmati, A. Keshavarz, Dual variable decomposition to discriminate the cost imposed by inflexible units in electricity markets, Appl. Energy (2021) 287.
[35] M. Azimian, V. Amir, R. Habibifar, H. Golmohamadi, Probabilistic optimization of networked multi-carrier microgrids to enhance resilience leveraging demand response programs, Sustainability 13 (11) (2021) 5792.